Imperial College London

CMTH-Vvedensky-3

Imperial College London

Department of Physics

A group-theoretical treatment of first-order perturbations of potential boundaries in semiconducting nanocrystals

Author:
Michal Horanský

Supervisor:
Dimitri D. Vvedensky

Assessor:
Jing Zhang

Word count: 2450

Date: April 19, 2024

1 Layperson's summary

Breaking the Symmetry, or, When Crystals Are Almost Perfect

The title of the layperson's summary: "Breaking the Symmetry, or, When Crystals Are Almost Perfect". It will focus firstly on the role of symmetries in selection rules and secondly on the overlap decomposition as a quantifier of what we mean by *approximate*. Technicalities such as double groups or growth of QDs shall be omitted for brevity (although [3] will be discussed as a motivator for the perturbative approach).

2 Abstract

In this project, we investigate the photonic properties of quantum dots employing a group-theoretical description of first-order perturbation theory. Experimental data from polarisation resolved photoluminiscence spectroscopy are investigated using the theory of exciton complexes and group theory. The major features of the spectral diagrams can be labelled by exciton state transitions immediately by considering the total angular momentum coupling of these exciton complexes. These major features also exhibit splitting caused by crystallographic symmetry breaking. The transitions between said energy levels are subject to symmetry selection rules, and we attempt to quantify the rates of these transitions by considering approximate symmetries. A list of other effects that may cause symmetry elevation is stated and reviewed.

3 Contents

4 Introduction

Firstly, a historical context of the problem and a brief literature review (namely [1]). Secondly, a brief review of [3] as a *de facto* solution to symmetry elevation, and then motivating the need for a perturbative analysis under strain and imperfect growth, which favour the three pyramid-defined directions out of the six grown. Thirdly, a list of proposed solutions, with the first one, a perturbative model of a low-symmetry Hamiltonian being mathematically explored and quantified.

5 Discussions of theory employed

5.1 The InGaAs pyramidal quantum dot

A brief description of the growth process as employed by Karlsson, Pelucchi etc. A discussion of [3] and its arguments for the true shape. A review of effects that alter the shape (and hence the symmetry) of a quantum dot, including strain and other mechanical effects.

5.2 Exciton complexes and double groups

The physical phenomenon which is subject to our study is photoluminiscence. Since this mechanism does not have the QDs in a laboratory ensemble interact or "communicate", we can formulate a theoretical model of photoluminiscence on a singular QD. An external electromagnetic field in the form of a light-beam interacts with the QD in a non-resonant way (as for not to favour a single excited state), which promotes electrons into the conduction band and holes into the valence bands (since there are typically two valence bands at the band edge, which touch at Γ). The population of excited electrons and different characteristics of holes is called an exciton complex. Exciton complexes decay into lower-occupancy exciton complexes via electron-hole recombination, which produces bright emission lines in the photoluminiscence spectrum. These lines are sharp and occur at fixed frequencies corresponding to the energy level differences, and the theoretical description of their spectrum is the ultimate goal of this work.
Exciton complexes are labelled by the number of electron-hole pairs and the occupancy numbers of each hole type. For example, $2X_{21}^{+}$ has 2 electrons, 2 heavy holes, 1 light hole, and an overall charge of $+1e$.
In the Karlsson *et al.* system, the light-beam is a laser with a spot size of $1\,\mu\mathrm{m}$, power in the range 25–$750\,\mathrm{nW}$, and wavelength of $532\,\mathrm{nm}$. The semiconductor nanocrystal has a direct band-gap at Γ. The excitons with resolvable emissions have low occupancy numbers (3 or fewer of any of the three fermions–electrons, light holes, and heavy holes). Since the number of fermions excited on a single band is smaller than the number of states available on the band by many orders of magnitude (GIVE ROUGH ESTIMATE), we approximate the exciton complexes as living on Γ, i.e. each excited fermion having zero crystal momentum.
INSERT BAND STRUCTURE DIAGRAM HERE
Clearly, the phenomenon of photoluminiscence and its behaviour is wholly described by the specific wavefunctions of the exciton complexes. However, finding the wavefunctions and the matrix elements of interaction operators is a near-impossible task and is not viable to make predictions about the spectrum of the quantum dot. However, we can make multiple very strong qualitative predictions (mainly regarding degeneracies of energy levels and selection rules) by using purely symmetry arguments, using the formalism of group theory. To employ group theory, we must first identify the physical symmetries of our quantum dot.

5.2.1 Envelope function method

The following approach is informed by that developed by Burt (1999), [6]. Let us consider a QD with a single excited electron which is promoted to the conduction band (the following easily generalises to holes promoted to valence bands). Disregarding the spin component of its wavefunction for simplicity, we decompose the electron's spatial wavefunction $\Psi\left(\vec{r}\right)$ into plane-waves:

$$\Psi\left(\vec{r}\right)=\int \mathrm{d}\vec{k}\tilde{\Psi}\left(\vec{k}\right)\exp\left\{i\vec{k}\cdot\vec{r}\right\} \tag{1}$$

where $\tilde{\Psi}\left(\vec{k}\right)$ is the Fourier transform of $\Psi\left(\vec{r}\right)$. We now decompose the integral domain into the first Brillouin zone (B.Z.) summed over the set of reciprocal lattice vectors G:

$$\Psi\left(\vec{r}\right)=\sum_{\vec{g}\in G}\int_{\vec{k}\in\text{1st B.Z.}}\mathrm{d}\vec{k}\tilde{\Psi}\left(\vec{k}+\vec{g}\right)\exp\left\{i\left(\vec{k}+\vec{g}\right)\cdot\vec{r}\right\} \tag{2}$$

Note that G is equivalent to the set of wave-vectors of plane waves periodic on the Bravais lattice. Therefore, we can choose a set of basis functions $U_n\left(\vec{r}\right)$ periodic on the Bravais lattice like so:

$$U_n\left(\vec{r}\right) = \sum_{\vec{g}\in G}u_n\left(\vec{g}\right)\exp\{i\vec{g}\cdot\vec{r}\} \tag{3}$$

$$U_n\left(\vec{r}+\vec{r}_B\right) = \sum_{\vec{g}\in G}u_n\left(\vec{g}\right)\exp\{i\vec{g}\cdot\vec{r}\}\exp\{i\vec{g}\cdot\vec{r}_B\}=U_n\left(\vec{r}\right) \tag{4}$$

where $\vec{r}_B\in R$ is a lattice vector and $u_n\left(\vec{g}\right)$ are the coefficients of the decomposition of U_n into reciprocal lattice plane waves, typically chosen such that U_n are orthonormal. Then, inverting this decomposition, we obtain

$$\exp\{i\vec{g}\cdot r\}=\sum_n u_n\left(\vec{g}\right)^* U_n\left(\vec{r}\right) \tag{5}$$

which allows us to decompose the original wavefunction into a sum of the orthonormal basis vectors U_n and their envelope functions Υ_n:

$$\Psi\left(\vec{r}\right) = \sum_n \Upsilon_n\left(\vec{r}\right)U_n\left(\vec{r}\right) \tag{6}$$

$$\Upsilon_n\left(\vec{r}\right) = \sum_{\vec{g}\in G}\int_{\vec{k}\in\text{B.Z.}}\mathrm{d}\vec{k}u_n\left(\vec{g}\right)^*\tilde{\Psi}\left(\vec{k}+\vec{g}\right)\exp\left\{i\vec{k}\cdot\vec{r}\right\} \tag{7}$$

Now, we choose $U_n\left(\vec{r}\right)$ to represent the band-edge wavestates in the bulk structure. Using a tight-binding model with spin-orbit coupling, these wavestates can be labelled by three quantum numbers: total angular momentum j, its projection onto the z-axis j_z, and the orbital energy excitation ε_n, which we assume to be in the ground state in our system due to energy occupancy statistics (as we expect the population of states other than in the ground state to be negligible for a low-power light-source). Furthermore, the quantum number j is determined by the orbital

angular momentum l, which is given by the electron configuration in each specific band, and the spin $s = 1/2$ determined for electrons and electron holes by their fundamental properties.
Photonic nanostructures can, on a small scale, cease to posses a standard band-structure, instead featuring e.g. flat bands. Dresselhaus *et al.* (2007) quotes the number of Bravais lattice cells below which this occurs to be in the order of 10^2 [11, p. 213]. Our QDs have volumes typically higher than $100\,\mathrm{nm}^3$ [2, p. 2], which corresponds to the number of unit cells in the order of 10^3. Hence we can reasonably expect our system to posses a band structure. This has two consequences to our envelope function model:

1. The envelope function $\Upsilon(\vec{r})$ is varying slowly enough for it to have an approximately defined crystal momentum. As discussed in 5.2, we assume $k \approx 0$.

2. The wavefunction $\Psi(\vec{r})$ of a single excited fermion approximately corresponds to a single state on the excited band of the infinite bulk crystal band structure. In other words, there exists a basis vector U_n such that for all other basis vectors $U_m, m \neq n$, their contribution to the wavefunction is negligible.

Labelling the single contributing basis vector by the quantum numbers l, s, j, j_z, we can express the wavefunction of a single excited fermion as

$$\langle \vec{r}|\Psi\rangle = \Upsilon(\vec{r})\,\langle \vec{r}|l, s = 1/2, j, j_z\rangle \tag{8}$$

As discussed in Burt (1992) [5, p. 6656], we can write down the effective Hamiltonian for the envelope function, which yields the corresponding Schrödinger equation:

$$\hat{H}_\Upsilon = -\frac{\hbar^2}{2}\nabla \cdot \frac{1}{m^*(\vec{r})}\nabla + E_0 \tag{9}$$

$$\hat{H}_\Upsilon \Upsilon(\vec{r}) = E\Upsilon(\vec{r}) \tag{10}$$

where E_0 is the band-edge energy. Now, in a parabolic Taylor expansion of the bands about Γ, we state that around the Γ point the effective mass m^* is constant. We now see that the Schrödinger equation reduces to the following form:

$$-\frac{\hbar^2}{2m^*}\nabla^2\Upsilon = (E - E_0)\Upsilon \tag{11}$$

This is the equation of a free particle with energy $E_p = E - E_0$. Hence we can model a single excited fermion as a "particle in a box" around the Γ point for a large enough structure.
Now we consider the wavefunction of an exciton complex, which is comprised of multiple excited fermions. The interaction between the fermions is purely electromagnetic. Since the envelope functions are slowly-varying and associated to zero crystal momenta, their magnetic interaction is negligible. The magnetic interaction of the periodic basis functions gives rise to spin-orbit and orbit-orbit coupling (ignoring the hyperfine structure of spin-spin coupling), which allows us to label an

exciton complex with a total angular momentum J and its projection onto the z-axis J_z as two quantum numbers. The Coulomb interaction between fermions a and b gives rise to a term in the Hamiltonian in the form

$$\hat{V}_{ab}^{C}\left(\vec{r}_a, \vec{r}_b\right) = \frac{q_a q_b}{4\pi\epsilon_0} \frac{1}{\left|\vec{r}_a - \vec{r}_b\right|} \tag{12}$$

This operator can be rewritten as a function of a single vector:

$$\hat{V}_{ab}^{C}\left(\vec{\xi}\right) = \frac{q_a q_b}{4\pi\epsilon_0} \frac{1}{\xi}, \qquad \xi = \left|\vec{\xi}\right| \tag{13}$$

Note that when this operator acts on the full two-particle wavefunction:

$$\hat{V}_{ab}^{C}\left(\vec{r}_a - \vec{r}_b\right) \Upsilon_a\left(\vec{r}_a\right) U_a\left(\vec{r}_a\right) \Upsilon_b\left(\vec{r}_b\right) U_b\left(\vec{r}_b\right) \tag{14}$$

the envelope functions Υ_a, Υ_b are slowly-varying, so we can state that they don't change in the volume of a single crystal lattice cell. Therefore, we can take the envelope functions outside of an integral where each vector $\vec{r}_a, \vec{r}_b$ is confined to a single cell:

$$\int_{\vec{r}_a \in \text{cell a}} \mathrm{d}^3\vec{r}_a \int_{\vec{r}_b \in \text{cell b}} \mathrm{d}^3\vec{r}_b \hat{V}_{ab}^{C}\left(\vec{r}_a - \vec{r}_b\right) \Upsilon_a\left(\vec{r}_a\right) U_a\left(\vec{r}_a\right) \Upsilon_b\left(\vec{r}_b\right) U_b\left(\vec{r}_b\right) \approx$$
$$\Upsilon_a\left(\vec{r}_a\right) \Upsilon_b\left(\vec{r}_b\right) \int_{\vec{r}_a \in \text{cell a}} \mathrm{d}^3\vec{r}_a \int_{\vec{r}_b \in \text{cell b}} \mathrm{d}^3\vec{r}_b \hat{V}_{ab}^{C}\left(\vec{r}_a - \vec{r}_b\right) U_a\left(\vec{r}_a\right) U_b\left(\vec{r}_b\right)$$

and since U_a, U_b are periodic over the crystal lattice, we can denote $\xi = \vec{R}_{\text{cell b}} - \vec{R}_{\text{cell a}}$ to be the lattice vector equal to the displacement between the two cells, then the integral becomes

$$\int_{\vec{r}_a \in \text{cell a}} \mathrm{d}^3\vec{r}_a \int_{\vec{r}_b \in \text{cell b}} \mathrm{d}^3\vec{r}_b \hat{V}_{ab}^{C}\left(\vec{r}_a - \vec{r}_b\right) \Upsilon_a\left(\vec{r}_a\right) U_a\left(\vec{r}_a\right) \Upsilon_b\left(\vec{r}_b\right) U_b\left(\vec{r}_b\right) \approx$$
$$\Upsilon_a\left(\vec{r}_a\right) \Upsilon_b\left(\vec{r}_b\right) \int_{\vec{r}_a \in \text{U.C.}} \mathrm{d}^3\vec{r}_a \int_{\vec{r}_b \in \text{U.C.}} \mathrm{d}^3\vec{r}_b \hat{V}_{ab}^{C}\left(\vec{r}_a - \vec{r}_b - \vec{\xi}\right) U_a\left(\vec{r}_a\right) U_b\left(\vec{r}_b\right)$$

where U.C. denotes a single unit cell of the crystal lattice centered around the origin (or otherwise fixed in space). Now comes the final approximation. When considering the integral of the expression 14 over an arbitrary dual volume, we partition the volumes into unit cells of the crystal lattice and then divide the integral into pairwise U.C.-U.C. integrals over a set of displacement vectors $\vec{\xi}$. For the majority of these vectors in dual volumes comparable in size to the size of the QD, the values of ξ will be larger than the dimensions of U.C. Hence we can approximate

$$\hat{V}_{ab}^{C}\left(\vec{r}_a - \vec{r}_b - \vec{\xi}\right) \approx \hat{V}_{ab}^{C}\left(\vec{\xi}\right) \tag{15}$$

By denoting the set of lattice vectors in the volume V as R_V, the integral simplifies to

$$\int_V \mathrm{d}^3\vec{r}_a \int_V \mathrm{d}^3\vec{r}_b \hat{V}_{ab}^{C}\left(\vec{r}_a - \vec{r}_b\right) \Upsilon_a\left(\vec{r}_a\right) U_a\left(\vec{r}_a\right) \Upsilon_b\left(\vec{r}_b\right) U_b\left(\vec{r}_b\right) \approx$$

$$\Pi_{ab} \sum_{\vec{r}_a \in R_V} \sum_{\vec{r}_b \in R_V} \hat{V}_{ab}^C \left(\vec{r}_a - \vec{r}_b\right) \Upsilon_a \left(\vec{r}_a\right) \Upsilon_b \left(\vec{r}_b\right)$$

where $\Pi_{ab} = \int_{\vec{r}_a \in \text{U.C.}} \mathrm{d}^3 \vec{r}_a \int_{\vec{r}_b \in \text{U.C.}} \mathrm{d}^3 \vec{r}_b U_a \left(\vec{r}_a\right) U_b \left(\vec{r}_b\right)$ is a correlation constant.

Now we renormalize the correlation constant Π_{ab} using the volume of the unit cell $V_{\text{U.C.}}$, which allows us to rewrite the double sum over R_V as an integral over the dual volume:

$$\int_V \mathrm{d}^3 \vec{r}_a \int_V \mathrm{d}^3 \vec{r}_b \hat{V}_{ab}^C \left(\vec{r}_a - \vec{r}_b\right) \Upsilon_a \left(\vec{r}_a\right) U_a \left(\vec{r}_a\right) \Upsilon_b \left(\vec{r}_b\right) U_b \left(\vec{r}_b\right) \approx$$
$$\Pi'_{ab} \int_V \mathrm{d}^3 \vec{r}_a \int_V \mathrm{d}^3 \vec{r}_b \hat{V}_{ab}^C \left(\vec{r}_a - \vec{r}_b\right) \Upsilon_a \left(\vec{r}_a\right) \Upsilon_b \left(\vec{r}_b\right),$$
$$\text{where} \quad \Pi'_{ab} = V_{\text{U.C.}}^{-2} \Pi_{ab} = \left\langle U_a \left(\vec{r}_a\right) U_b \left(\vec{r}_b\right) \right\rangle_{\text{U.C.}}$$

Since this must be true for any (sufficiently large) V, we drop the integral altogether, equating the integrands:

$$\hat{V}_{ab}^C \left(\vec{r}_a - \vec{r}_b\right) \Psi_a \left(\vec{r}_a\right) \Psi_b \left(\vec{r}_b\right) = \Pi'_{ab} \hat{V}_{ab}^C \left(\vec{r}_a - \vec{r}_b\right) \Upsilon_a \left(\vec{r}_a\right) \Upsilon_b \left(\vec{r}_b\right) \quad \text{on vol. avg.} \tag{16}$$

What was done here was essentialy taking a volume average over the product of the basis functions $U_a U_b$, motivated by their periodicity over unit volumes much smaller than that of the quantum dot. This high-frequency periodicity manifests as a simple correlation coefficient when considering matrix elements of $\hat{V}_{ab}^C$.
This allows us to modify 11 to account for Coulomb interaction purely in the paradigm of envelope functions. The full effective Schrödinger equation for envelope functions (since the fine structure effects do not matter for the slowly-varying envelope functions) is then

$$\left(-\sum_i \frac{\hbar^2}{2m_i^*} \nabla_{\vec{r}_i}^2 + \sum_{i,j;i \neq j} \Pi'_{ij} \hat{V}_{ij}^C \left(\vec{r}_i - \vec{r}_j\right) \right) \Upsilon = E_{\text{exciton}} \Upsilon \tag{17}$$

where

$$\Upsilon = \prod_i \Upsilon_i \left(\vec{r}_i\right)$$

Note that the Coulomb interaction on the volumes of the scale of the unit cell of the crystal lattice is fully rotationally symmetric, and therefore will not invalidate J, J_z as good quantum numbers. However, it will affect the value of Π'_{ij}, which therefore becomes nontrivial to calculate. It will also affect the shape of the periodic functions, which we can for simplicity just denote $F_i \left(\vec{r}_i\right)$, and which have the same periodic properties as $U_i \left(\vec{r}_i\right)$, and form in totality a J, J_z eigenstate. Therefore, we expect the transformation $U_i \to F_i$ to only affect the radial dependence in the close vicinity of an atom, preserving the spherical-harmonics angular dependence in the tight-binding model.
By interpreting eq. 17, we now see that the envelope functions in an exciton complex behave as free particles in a box with added Coulomb interactions, i.e. a many-body

charged particle system. Note that the potential barriers at the edges of the "box" are not infinite, and that would indeed not be a good approximation!
Note. Even though $\hat{V}_{ab}^{C}\left(\vec{r}_a - \vec{r}_b\right)$ diverges for $\vec{r}_a = \vec{r}_b$ (which occurs in the small subset of $R_V \otimes R_V$ where both vectors are in the same unit cell), the contribution of the integrals over these coinciding unit cells should not be disproportionally high, since when considering the volume integral in spherical coordinates centered on the asymptote, the integrand goes like $|\vec{r}_a - \vec{r}_b|$, so the integral should be approximately proportional to $V_{\text{U.C.}}^{2/3}$, and the contribution from this subset where our approximations fail to the total integral is negligible.

5.2.2 Symmetry arguments, group theory, and double groups

Now that we have decomposed the single excited fermion wavefunction into a j-eigenstate periodic in the atomic lattice and a slowly varying envelope function which corresponds to a zero bulk-crystal momentum, we turn to symmetry arguments to make predictions about the spectrum. Indeed, finding either of the two component functions is a task beyond the scope of this work, but we can make quantitative statements about the splitting of the exciton energy levels and selection rules for transitions between these energy levels. To do this, we must consider how the exciton wavefunction transforms under symmetry transformations of the true Hamiltonian.
To review the basic applications of group theory to quantum mechanics as outlined e.g. in Dresselhaus (2002) [12], we consider the set of rotations commuting with a Hamiltonian $\hat{H}$. This set forms a group under multiplication (as for $\hat{R}_1, \hat{R}_2$ commuting with $\hat{H}$, $\hat{R}_1\hat{R}_2$ must be a single rotation $\hat{R}_3$ which also commutes with $\hat{H}$). This group shall be denoted as $G_{\hat{H}}$, and is referred to as the group of the Hamiltonian. As shown in standard texts, each energy level E_n of the time-independent Schrödinger eigenvalue problem $\hat{H}\Psi_n = E_n\Psi_n$ corresponds to an irreducible representation (irrep) of $G_{\hat{H}}$, which we can denote as $\Gamma_{r(n)}$, where r is some mapping. The degeneracy of E_n is then equal to the dimension of $\Gamma_{r(n)}$. Therefore, knowing the group of the Hamiltonian tells us the possible degeneracies of the energy levels and what they transform like under the symmetry transformations.
Moreover, group theory has an application to selection rules. Consider two energy levels E_a, E_b of a system with the Hamiltonian $\hat{H}$. If we add a perturbation $\hat{H}'$ which allows transition between energy levels, and which transforms according to the representation $\Gamma_{\hat{H}'}$, by Fermi's golden rule the rate of transition $E_a \to E_b$ is proportional to the matrix element $\langle E_a|\hat{H}'|E_b\rangle$ (if the energy levels are degenerate, we need to pick a set of basis vectors and consider the rates of transition between each pair of basis vectors). As per [12, Ch. 7], this matrix element vanishes if the irrep direct product $\Gamma_{r(a)} \otimes \Gamma_{\hat{H}'} \otimes \Gamma_{r(b)}$ does not contain the identity representation. This allows us to decide which exciton transitions under photoluminiscent electron-hole recombination will be dark in which polarisation.
Consider now the effective Hamiltonians acting on the envelope function $\Upsilon = \prod_i \Upsilon_i\left(\vec{r}_i\right)$ and the periodic function $F = \prod_i F_i\left(\vec{r}_i\right)$, respectively.

1. Υ, representing a many-body charged particle-in-a-box system, is governed in

its symmetry by the shape of the box, i.e. the shape of the QD. In our system, this shape is assumed to posses C_{3v} (tetrahedral) symmetry. This symmetry shall be referred to as the *structure symmetry*.

2. F, representing a function periodic in the crystal lattice, is governed in its symmetry by the shape of the lattice, i.e. the properties of the bulk of the crystal. In our system, the crystal lattice is a zincblend structure (cubic FCC) around the [111] direction. The point group of this lattice is T_d. This symmetry shall be referred to as the *bulk symmetry*.

3. Around the individual atoms in the crystal lattice, in the tight-binding model the exciton forms a total angular momentum eigenstate $|J, J_z\rangle$. This has a full roto-inversion symmetry, and since it is a spin-half spinor, the group describing the full roto-inversion symmetry is $SU(2) \otimes C_i$, where $C_i = \{\hat{E}, \hat{i}\}$ is the inversion group and it is isomorphic to $\mathbb{Z}_2$.

Naturally, the symmetry of the true Hamiltonian will be the lowest one of these, which is in our case the structure symmetry C_{3v}–or rather, since we are discussing spin-half spinors, its double group, as will be discussed below. However, as we argue below, the bulk symmetry will be important when explaining the origin of symmetry elevation in our perturbative model.
Now, let us consider the character of the full exciton wavefunction under a symmetry transformation $\hat{R}$. Since the Coulomb interaction transforms according to the identity rep under roto-inversions, we can first consider the character of a single fermion wavefunction under the symmetry transformation, and then we construct the full exciton character through j-coupling, as discussed in Sec. 5.2.3. Since the single excited fermion wavefunction is a product of two functions, its character will be the product of the two constituent characters:

$$\chi^{(\Psi(\vec{r}))}\left(\hat{R}\right) = \chi^{(\Upsilon(\vec{r}))}\left(\hat{R}\right)\chi^{(U(\vec{r}))}\left(\hat{R}\right) \tag{18}$$

The character of the envelope function can be, in principle, any irrep of the structure symmetry group. However, we once again invoke the energy statistics–the population of QDs excited by a low-energy laser for which the envelope functions are out of the ground state should be negligible. Therefore, assuming the envelope function is in its ground state, we know it transforms according to the identity rep. Therefore $\chi^{(\Upsilon(\vec{r}))}\left(\hat{R}\right) = 1$.
In the tight-binding model, the band-edge eigenstate U is a convolution of the j-eigenstate which exists around each atom with the distribution of the atoms, weighted relatively to their atomic properties. Since the structure symmetry group is a subgroup of the bulk symmetry group, the bulk crystal lattice maps onto itself under every rotation in the structure symmetry. Furthermore, the Ga-As bonds in the conduction band are antisymmetric, and the second-nearest neighbour bonds are symmetric [7], which leaves the lattice to transform according to the identity rep. (FIGURE HERE)
Therefore the only part of the single excited fermion wavefunction which does not necessarily transform according to the identity rep is the j-eigenstate itself. The

character of a j-eigenstate is just the trace of the corresponding Wigner D-matrix (CITATION), and each set of eigenstates

$$\begin{pmatrix} |j, j_z = j\rangle \\ |j, j_z = j-1\rangle \\ \vdots \\ |j, j_z = -j\rangle \end{pmatrix} \text{ forms a basis to } \Gamma_j^{(SU(2))}$$

To extend this unto roto-inversions, we need to consider the orbital angular momentum l, which determines inversion parity. For example, in our system, the conduction band is an s-orbital, which has even parity under inversion, but the valence band is a p-orbital, which has odd parity under inversion. Determining parity specifies the irrep of the full roto-inversion group $SU(2) \otimes C_i$, which gains an index g (gerade) if even or u (ungerade) if odd under inversion.
Our approach to construct the transformation laws for the single excited fermions is therefore to consider the irreps of the full roto-inversion spinor group, and then decompose them into the true symmetry, i.e. the structure symmetry. To do this, we must construct the double group of the structure symmetry point group. Essentially, a double group encodes the spin-orbit coupling for its original group by adding the time-reversal operator as a generator. This renders rotations by 2π to result in time-reversal, and only rotations by 4π return back to the identity, in agreement with the behaviour of spin-half particles under rotation. The theory of double groups is outlined in [12, Ch. 19], and the character tables of double groups can be found in standard tables, such as [14].
Applying this approach, we find that an electron promoted to the s-orbital conduction band transforms according to $\Gamma_{j=1/2,g}$ in the full roto-inversion group, which reduces to $E_{1/2}$ in the C_{3v} double group. Conversely, a hole promoted to the p-orbital valence band transforms according to $\Gamma_{j=1/2,u} \oplus \Gamma_{j=3/2,u}$ in the full roto-inversion group. We identify $\Gamma_{j=1/2,u}$ as the split-off band which has lower energy at the band-edge, and hence will not be populated in our system. Conversely, $\Gamma_{j=3/2,u}$ decomposes into $E_{1/2} \oplus E_{3/2}$ in the C_{3v} double group, where $E_{1/2}$ corresponds to the light-hole band ($j_z = \pm 1/2$) and $E_{3/2}$ corresponds to the heavy-hole band ($j_z = \pm 3/2$). This also illustrates the symmetry-informed reason why there are two different hole types.

5.2.3 Total angular momentum coupling and Pauli's exclusion principle

To obtain the transformation properties of an exciton complex, we must consider the magnetic orbit-orbit and spin-orbit interaction which couples the total angular momenta j of separate fermions together. The treatment of j-coupling in the full roto-inversion symmetry is as follows:
Consider two non-interacting particles governed by Hamiltonians which conserve total angular momentum. Let the two particles exist in j-eigenstates $\left|j^A, j_z^A, p\right\rangle, \left|j^B, j_z^B, p\right\rangle$ respectively (here p specifies the inversion parity), and the group of each of their Hamiltonians is $SU(2) \otimes C_i$. The full Hilbert space they occupy is the direct product of the Hilbert space occupied by each particle, and hence the group of the total

Hamiltonian is:

$$G_{\hat{H}}^{\text{nonint.}} = (SU(2) \otimes C_i) \otimes (SU(2) \otimes C_i) \tag{19}$$

The irreps of this group are the direct products of the respective irreps $\Gamma_{j,p}$, and hence

$$\left|j^A, j_z^A, p^A\right\rangle \otimes \left|j^B, j_z^B, p^B\right\rangle \quad \text{transforms according to} \quad \Gamma_{j^A,p^A} \otimes \Gamma_{j^B,p^B} \tag{20}$$

If we now include an interaction term in the full Hamiltonian which couples the total angular momenta of the particles, j_z^A, j_z^B cease to be good quantum numbers. Instead (in classic electromagnetic coupling), the full total angular momentum J and its projection along the z-axis, J_z, become good quantum numbers. Preserving j^A, j^B as immutable parameters of the physical system, the new energy eigenstates posses the roto-inversion symmetry $SU(2) \otimes C_i$, and transform according to its irreps–this is determined wholly by the quantum numbers, which specify the partitioning of the Hilbert space into degenerate subspaces. Hence we need to reduce the high-symmetry irrep in Eq. 20 into the lower-symmetry group $SU(2) \otimes C_i$.
A decomposition is always unique by the Great Orthogonality Theorem (CITATION), therefore finding a decomposition is sufficient to prove it is the correct one. We will assume that all constituent irreps in the decomposition have equal parity, which is the product of the two parities $p^A \cdot p^B$. Then, using standard results (CITATION), we write down the decomposition:

$$\Gamma_{j^A,p^A} \otimes \Gamma_{j^B,p^B} = \sum_{J=|j^A-j^B|}^{j^A+j^B} \Gamma_{J,p^A \cdot p^B} \tag{21}$$

We can now generalise this approach to cases where each particle's original Hamiltonian undergoeas symmetry breaking to some double group $\tilde{G}_{\hat{H}_0}$, which is a subgroup of $SU(2) \otimes C_i$. In the non-interacting direct product of the two Hilbert spaces, each pair of quantum numbers j^i, j_z^i reduces into an instance of this subgroup, and so the pair of non-interacting particles transforms according to $\tilde{G}_{\hat{H}_0} \otimes \tilde{G}_{\hat{H}_0}$. If we include the j-coupling interaction term, the full system features only one pair of these quantum numbers, J, J_z, which reduce into a single instance of the aforementioned subgroup. Hence, the reduction goes like this:

$$\Gamma_A^{\left(\tilde{G}_{\hat{H}_0}\right)} \otimes \Gamma_B^{\left(\tilde{G}_{\hat{H}_0}\right)} \to \bigoplus_i \Gamma_i^{\left(\tilde{G}_{\hat{H}_0}\right)} \tag{22}$$

Naturally, as the constituent irreps in the direct sum on the right side correspond to different energy levels (disregarding accidental degeneracy), the symmetry breaking associated with coupling of quantum numbers lowers the degeneracy of the system. The outlined method is sufficient for finding the energy levels of distinguishable particles undergoing coupling; however, in our case, the particles are fermions, and hence, for particles occupying the same k-state in the same band, we also have to consider Pauli's exclusion principle.
The conduction band is an s-orbital, and hence the excited electrons have $j = 1/2$, which renders their k-states doubly degenerate. The valence band is a p-orbital, and

hence the holes have $j = 3/2$ and 4-fold degenerate k-states. However, for most groups, including C_{3v}, the $SU(2) \otimes C_i$ irrep $\Gamma_{j=3/2,u}$ reduces to two 2-dimensional irreps, which causes the holes to have two different characters (light-like and heavy-like), each with doubly degenerate k-states. We assume that the bands fill up sequentially under excitation in a way that maximises the number of completely filled-out states.

- For doubly degenerate k-states, we only need to find the transformation properties of the full k-state, i.e. a pair of fermions. As per Karlsson *et al.* [1, p. 15], a full doubly degenerate energy level transforms according to the identity representation.

- For 4-fold degenerate k-states with $j = 3/2$, we can extend Karlsson's argument to claim that the full energy level with 4 particles transforms according to the identity representation. We can label an energy level with 3 particles by the 1 missing particle, and hence it transforms equally to an energy level filled with 1 particle. Finally, for two particles, we need to construct the 6 antisymmetric basis vectors, with kets labelled by the j_z values of the first and the second particle respectively:

$$\begin{aligned} b_1 &= \tfrac{1}{\sqrt{2}}\left(\left|\tfrac{3}{2},-\tfrac{3}{2}\right\rangle - \left|-\tfrac{3}{2},\tfrac{3}{2}\right\rangle\right) & b_2 &= \tfrac{1}{\sqrt{2}}\left(\left|\tfrac{1}{2},-\tfrac{1}{2}\right\rangle - \left|-\tfrac{1}{2},\tfrac{1}{2}\right\rangle\right) \\ b_3 &= \tfrac{1}{\sqrt{2}}\left(\left|\tfrac{3}{2},\tfrac{1}{2}\right\rangle - \left|\tfrac{1}{2},\tfrac{3}{2}\right\rangle\right) & b_4 &= \tfrac{1}{\sqrt{2}}\left(\left|-\tfrac{3}{2},-\tfrac{1}{2}\right\rangle - \left|-\tfrac{1}{2},-\tfrac{3}{2}\right\rangle\right) \\ b_5 &= \tfrac{1}{\sqrt{2}}\left(\left|\tfrac{3}{2},-\tfrac{1}{2}\right\rangle - \left|-\tfrac{1}{2},\tfrac{3}{2}\right\rangle\right) & b_6 &= \tfrac{1}{\sqrt{2}}\left(\left|-\tfrac{3}{2},\tfrac{1}{2}\right\rangle - \left|\tfrac{1}{2},-\tfrac{3}{2}\right\rangle\right) \end{aligned}$$

  The character of a rotation is given purely by the angle θ, not by the rotation axis, as

$$\chi^{(\Gamma_j)}\left(\hat{R}(\theta)\right) = \frac{\sin\left(2j+1\right)\theta/2}{\sin\theta/2} \tag{23}$$

  which is just the trace of the Wigner d-matrix, which Wigner defined as

$$d^j_{m',m} = \langle j, m'|\hat{R}(\theta)|j, m\rangle \tag{24}$$

  where θ is the second Euler angle in the z-y-z convention [8, p.160], and for which Wigner gave an expression [8, p.167]. The character of a simultaneous rotation of two particles is a product of the two single-particle rotation characters, which allows us to calculate the sum of the simultaneous-rotation characters over all basis vectors:

$$\sum_{i=1}^{6} \chi^{b_i}\left(\hat{R}(\theta)\right) = 2\cos\theta + 2\cos 2\theta + 2 \tag{25}$$

  which we can equate to the sum of the characters of $\Gamma_{j=0} \oplus \Gamma_{j=2}$, as per eq. 23. Hence an energy level with $j = 3/2$ filled with two particles transforms as $\Gamma_{j=0} \oplus \Gamma_{j=2}$.

Hence we can label any exciton complex for groups which have one or two hole characters by labelling each fermion type by the number of free fermions and then multiplying the corresponding representations for each fermion type. Reducing this into the irreps of the structure symmetry group gives is the number of energy levels and their degeneracies for each exciton complex.

5.3 Photoluminiscence spectrum and evidence of symmetry elevation

To predict the rate of photoluminiscent transitions between energy levels, we utilize the dipole approximation, in which the dipole operator (and hence the perturbing Hamiltonian) transforms as a vector [1, p. 13]. Vectors transform according to the Cartesian representation, which can be easily constructed from rotation matrices [8, p. 160]. If the Cartesian representation is reducible in the structure symmetry group, different vector orientations of the dipole may transform differently, resulting in different lines in polarised spectra. In that case, we must apply the selection rules outlined in Sec. 5.2.2 for each polarisation separately. Then, the number of allowed transitions between different finely-split energy levels of two excitons gives the number of tightly-spaced lines we predict on the spectrum of that exciton transition.
In [1], Karlsson *et al.* have applied the selection rules to different exciton transitions and compared the predicted number of lines to their experimental data. (FIGURE HERE) The predictions have mostly agreed, but three exciton transitions were identified for which emission lines in the measured spectra were missing. These were:

1. $X_{10} \rightarrow$vacuum (2 predicted $x-y$-polarised lines, 1 measured).
2. $2X_{20} \rightarrow X_{10}$ (2 predicted $x-y$-polarised lines, 1 measured).
3. $2X_{11} \rightarrow X_{01}$ (6 predicted $x-y$-polarised lines, 3 resolved strongly and 2 more resolved weakly).

Karlsson *et al.* theorise that the missing lines or the relative intensity of lines in these transitions can be explained by a symmetry elevation to a larger group of symmetries which contains C_{3v}. In our work, we have attempted to test this claim.

6 Results–symmetry suppression theory

In our research, we tested the following hypothesis: *Symmetry elevation effects are caused by transformation properties of the bulk symmetry.* Since the bulk symmetry group T_d contains the structure symmetry C_{3v} as a subgroup, it is a natural suspect for a source of *approximate* symmetries, since it limits the true symmetry of the system.
The theoretical basis for particular excitons enjoying symmetry transformations from the bulk symmetry is built on their localisation within the QD. If the envelope functions Υ_i of every fermion in an exciton complex are localised near the centre of the QD, any bulk-symmetry transformation should also be a symmetry transformation of the exciton wavefunction. With every QD border the envelope functions approach, more approximate symmetry transformations vanish, until, when an exciton has significant probability to measure one or more of its fermions around the entire edge of the QD, it fully probes the structure symmetry.

6.1 Perturbative analysis of selection rules

Suppose now we have a system described by a Hamiltonian $\hat{H}$ equipped with a group of symmetries G. Let us construct a Hamiltonian $\hat{H}_+$ which is equipped with a group of symmetries G_+ such that $G < G_+$ and $\hat{H}$ can be modelled as a perturbation of $\hat{H}_+$ like so:

$$\hat{H} = \hat{H}_+ + \lambda\hat{H}', \quad \text{where} \quad \lambda \ll 1$$

For an exciton with its wavefunction localised in the centre of the QD, $\hat{H}$ is the true Hamiltonian, and $\hat{H}_+$ is the Hamiltonian of a smaller QD inscribed into the true QD with a higher symmetry.

6.1.1 Elevated symmetry component of an energy eigenstate

Let us denote the eigenstates of the Hamiltonians $\hat{H}, \hat{H}_+$ as $|E_i; n\rangle$ and $\left|E^+_{i'}; n'\right\rangle$ respectively, where n, n' are the degeneracy labels. Disregarding accidental degeneracy, we know that every set of degenerate energy levels forms a basis of (i.e. transforms according to) an irrep of the respective symmetry group:

$$\begin{pmatrix} |E_i;1\rangle \\ |E_i;2\rangle \\ \vdots \\ |E_i;d_i\rangle \end{pmatrix} \text{ forms a basis to } \Gamma^{(G)}_{r(i)}; \quad \begin{pmatrix} \left|E^+_{i'};1\right\rangle \\ \left|E^+_{i'};2\right\rangle \\ \vdots \\ \left|E^+_{i'};d^+_{i'}\right\rangle \end{pmatrix} \text{ forms a basis to } \Gamma^{(G_+)}_{r^+(i')}$$

where $d_i, d^+_{i'}$ specify the total degeneracies of the energy levels and r, r^+ are some functions which map energy levels onto irreps. Under a first-order perturbation of a set of degenerate eigenstates, the distance of the new states from the subspace $\mathcal{D}^+$ spanned by the degenerate eigenstates goes like $O(\lambda)$. Therefore, if $|E_i; n\rangle$ arises from perturbing a degenerate subspace of energy E^+_j, there exists an unnormalized

vector $\left|E_j^+;P\right\rangle \in \mathcal{D}_j^+$ for which

$$\begin{aligned} \frac{\left\langle E_i;n\middle|E_j^+;P\right\rangle}{\left|\left\langle E_j^+;P\middle|E_j^+;P\right\rangle\right|^{1/2}} &= 1-O(\lambda) \\ \text{where} \quad \left\langle E_j^+;P'\middle|E_i;n\right\rangle &= \left\langle E_j^+;P'\middle|E_j^+;P\right\rangle \quad \text{for all} \quad \left|E_j^+;P'\right\rangle \in \mathcal{D}^+ \end{aligned}$$

We can construct a state satisfying these conditions by projecting the perturbed eigenstate onto the original degenerate subspace:

$$\begin{aligned} \hat{P}_j^+ &= \sum_{m=1}^{d_j^+} \left|E_j^+;m\right\rangle\!\left\langle E_j^+;m\right| \\ \left|E_j^+;P\right\rangle &= \hat{P}_j^+\left|E_i;n\right\rangle = \sum_{m=1}^{d_j^+}\left|E_j^+;m\right\rangle\left\langle E_j^+;m\middle|E_i;n\right\rangle \end{aligned}$$

Now we can express a general eigenstate of $\hat{H}$ as a superposition of an eigenstate of $\hat{H}^+$ with a norm that goes like $1-O(\lambda)$ and a remainder. We normalize the components and introduce superposition coefficients:

$$\left|E_i;n\right\rangle = c_{ES}\left|E_j^+;ES\right\rangle + c_R\left|R\right\rangle \tag{26}$$

where the *elevated symmetry component* is defined as

$$\begin{aligned} \left|E_j^+;ES\right\rangle &= \left|E_j^+;P\right\rangle\left|\left\langle E_j^+;P\middle|E_j^+;P\right\rangle\right|^{-1/2} \\ &= \left|E_j^+;P\right\rangle\left(\sum_{m=1}^{d_j^+}\left|\left\langle E_j^+;m\middle|E_i;n\right\rangle\right|^2\right)^{-1/2} \\ c_{ES} &= \left\langle E_j^+;ES\middle|E_i;n\right\rangle \\ &= \sqrt{\sum_{m=1}^{d_j^+}\left|\left\langle E_j^+;m\middle|E_i;n\right\rangle\right|^2} \\ &\sim 1-O\left(\lambda\right) \end{aligned}$$

and the *residual component* then becomes

$$\left|R\right\rangle = c_R^{-1}\left(\left|E_i;n\right\rangle - c_{ES}\left|E_j^+;ES\right\rangle\right)$$

By demanding norm 1, we obtain:

$$\begin{aligned} 1 &= c_R^{-2}\left(\langle E_i;n|E_i;n\rangle + c_{ES}^2\left\langle E_j^+;ES\middle|E_j^+;ES\right\rangle - 2c_{ES}\left\langle E_i;n\middle|E_j^+;ES\right\rangle\right) \\ c_R &= \sqrt{1-c_{ES}^2} \\ &\sim O(\lambda) \\ \left|R\right\rangle &= \left(1-c_{ES}^2\right)^{-1/2}\left(\left|E_i;n\right\rangle - c_{ES}\left|E_j^+;ES\right\rangle\right) \end{aligned}$$

6.1.2 Selection rules for the elevated symmetry component

Consider now two eigenstates of $\hat{H}$ at different energy levels, $|E_i; n_i\rangle$, $|E_f; n_f\rangle$. If we perturb the system with an interaction Hamiltonian $\hat{H}'$, the rate of transition between these two states is given by Fermi's golden rule

$$\Gamma_{|E_i;n_i\rangle \to |E_f;n_f\rangle} = \frac{2\pi}{\hbar} \left| \langle E_f; n_f | \hat{H}' | E_i; n_i \rangle \right|^2$$

Since the energy levels may be degenerate, the full transition rate between the two sets of degenerate states becomes

$$\Gamma_{E_i \to E_f} = \sum_{n_i=1}^{d_i} \sum_{n_f=1}^{d_f} \Gamma_{|E_i;n_i\rangle \to |E_f;n_f\rangle}$$

Let the energy levels E_i, E_f be chosen such that the direct product $\Gamma^{(G)}_{r(i)} \otimes \Gamma^{(G)}_{\hat{H}'} \otimes \Gamma^{(G)}_{r(f)}$ contains the identity irrep of G, and hence the matrix elements do not vanish due to the selection rule. Let us now decompose the two eigenstates into elevated symmetry and residual components:

$$\begin{aligned} |E_i; n_i\rangle &= c^i_{ES} \left| E^+_{i'}; ES \right\rangle + c^i_R \left| R_i \right\rangle \\ |E_f; n_f\rangle &= c^f_{ES} \left| E^+_{f'}; ES \right\rangle + c^f_R \left| R_f \right\rangle \end{aligned}$$

where $E^+_{i'}, E^+_{f'}$ denote the energy levels of the high-symmetry Hamiltonian $\hat{H}^+$ which get perturbed into E_i, E_f respectively.
Let us now calculate the matrix element under the interaction Hamiltonian:

$$\begin{aligned} &\langle E_f; n_f | \hat{H}' | E_i; n_i \rangle = \\ &\left(c^f_{ES}\right)^* c^i_{ES} \left\langle E^+_{f'}; ES \middle| \hat{H}' \middle| E^+_{i'}; ES \right\rangle + \left(c^f_{ES}\right)^* c^i_R \left\langle E^+_{f'}; ES \middle| \hat{H}' \middle| R_i \right\rangle + \\ &\left(c^f_R\right)^* c^i_{ES} \left\langle R_f \middle| \hat{H}' \middle| E^+_{i'}; ES \right\rangle + \left(c^f_R\right)^* c^i_R \left\langle R_f | \hat{H}' | R_i \right\rangle \end{aligned}$$

We know that $\left(c^f_R\right)^* c^i_R$ goes like $O\left(\lambda^2\right)$, and hence we will disregard the corresponding term. There are now two possibilities for what may occur:

1. *The elevated symmetry matrix element does not vanish.* If $\Gamma^{(G_+)}_{r^+(i')} \otimes \Gamma^{(G_+)}_{\hat{H}'} \otimes \Gamma^{(G_+)}_{r^+(f')}$ contains the identity irrep of G_+, the leading term matrix element does not vanish, and forms the main contribution to the total matrix element.

2. *The elevated symmetry matrix element vanishes.* If $\Gamma^{(G_+)}_{r^+(i')} \otimes \Gamma^{(G_+)}_{\hat{H}'} \otimes \Gamma^{(G_+)}_{r^+(f')}$ does not contain the identity irrep of G_+, the leading term matrix element vanishes due to the selection rule (since it must transform as a scalar). The only non-zero terms are now the cross-terms, which both go like $O(\lambda)$, and the transition rate goes like $O(\lambda^2)$. Hence, even though these spectral lines are not fully forbidden by the selection rule, they are reduced by an order of magnitude (and vanish in first order) due to their high partial symmetry–this is symmetry suppression.

6.2 Localisation of pure-heavy-hole excitons in the bulk

The shape of the exciton wavefunctions is not well-understood, as calculating them is highly non-trivial. However, we can state qualitative arguments that describe the localisation of fermions in the QD approximately. For this, we will use the results from Sec. 5.2.1 to treat the fermion envelope functions Υ_i as a Coulomb-interacting many-body system in a finite potential well. This highly approximate method will provide the justification for our expectation of some excitons being highly localised in the bulk of the QD.

Firstly, for a single particle in a finite potential well, we shall inquire on the role of the effective mass m^* in the tunnelling of the wavefunction into the edges of the well, which probes the structure symmetry. As shown e.g. by Landau in [9, p. 64], the attenuation coefficient is proportional to $\sqrt{m^*}$ for 1D wells. This result is readily generalised for 3D systems of arbitrary shape, since in the region outside the well, the Schrödinger equation has the form

$$\left(\frac{\hat{p}}{\sqrt{2m^*}}\right)^2 |\Upsilon\rangle = (E - V)\,|\Upsilon\rangle \tag{27}$$

where $V > E$ is the depth of the potential well, larger than the particle energy, since the particle is constrained within the QD. We see that the sign of $E - V$ is negative. Since the particle is free in the regime outside of the potential well, we expect it to be (approximately) an eigenfunction of $\hat{p}$ as well as $\hat{H}$, especially if the shape of the potential well boundary in three dimensions is smooth. Then the eigenvalue of $\hat{p}$ must be purely imaginary to match the sign on both sides, and proportional to $\sqrt{m^*}$ for the attenuation coefficient in the spatial dependence to be of dimension m^{-1}. This allows us to conclude that fermions with high effective mass (such as heavy holes with $m^*_{hh} \approx 0.5 m_e$) will be more strongly localised in the centre of the QD bulk than fermions with low effective mass (such as electrons with $m^*_e \approx 0.059 m_e$ and light holes with $m^*_{lh} \approx 0.076 m_e$). *Note.* The effective masses were calculated for $In_{0.10}Ga_{0.90}As$ with the formulas provided by Goldberg and Schmidt in [10, p. 62]. These formulas are stated for $T = 300\,\mathrm{K}$, but we do not expect the effective masses to vary between $T = 30\,\mathrm{K}$ and $300\,\mathrm{K}$ significantly for this qualitative argumentation, as the fact that m^*_e and m^*_{lh} are of the same order of magnitude and m^*_{hh} is larger by an order of magnitude should remain true. This leads us to a hypothesis that single light holes and single electrons probe the structure symmetry, but single heavy holes are localised in the centre of the QD and undergo symmetry elevation to the bulk symmetry.

If we occupy the QD with two or more excited fermions of the same type, the total Hamiltonian will be invariant under exchanging any two of them, which implies a symmetry in the magnitude of Υ_i (the full spinor wavefunction, naturally, will be antisymmetric under exchange of two indistinguishable particles). This means every single particle in the equal-type fermionic complex either probes the structury symmetry or is localised in the centre. This means that multiple light holes and multiple electrons should both probe the structure symmetry under our previous assumptions, and we hypothesise that multiple heavy holes are still localised in the centre.

If we mix excited fermions of different types into exciton complex, we can now see the logical conclusions of our hypothesis. In excitons with only light holes, both the light holes and the excitons probe the structure symmetry and their Coulomb attraction does not affect that. In excitons with both light and heavy holes, the light holes still probe the structure symmetry, a phenomenon reinforced by their Coulomb repulsion with the centrally-localised heavy holes, which may push the light holes further out into the edges of the QD. Finally, in excitons with purely heavy holes, the Coulomb attraction between the heavy holes and the electrons increases the probability of measuring the electrons near the centre of the QD. Hence only purely heavy hole-like excitons undergo symmetry elevation to the bulk symmetry and enjoy symmetry suppression effects in this model.
Note. Since the shape of the envelope functions is not known, the fact that pure-light hole excitons probe the structure symmetry is empirical in our model.

6.3 Identifying intermediate groups of bulk and structure symmetries

Any symmetry transformation which is not a symmetry transformation of the crystal bulk is not a true symmetry transformation of the system [4]. Since every element of the structure symmetry G_s is also an element of the bulk symmetry G_b (which requires a specific orientation of the zincblende lattice), any candidate approximate symmetry G_a has to satisfy $G_s \subset G_a \subseteq G_b$. Consulting the group chains in [14, Ch.9], we see that there is only one group that satisfies this condition, which is the bulk symmetry group T_d itself. Our model of symmetry suppression therefore requires T_d to be the symmetry we elevate to.
In the analysis, we have also included the groups D_{3d}, and O_h as close supergroups of C_{3v}, as well as D_{3h}, the close supergroup of C_{3v} which Karlsson *et al.* claimed to match their experimental data for symmetry-elevated exciton decays, and which gives equal predictions to C_{6v}, another close supergroup [1, p. 19] .
Note that when making predictions for the bulk symmetry group T_d, at the $k = 0$ point (Γ) the light hole band and heavy hole band become degenerate (REF TO PREVIOUS FIG) and together they transform as a single four-dimensional irrep of T_d. This means that for groups such as T_d, O_h, or any groups containing these as subgroups, where no splitting between the four $j = 3/2$ states occurs, the predictions at the Γ point do not depend on the occupancy numbers of each type of hole, only their total sum.
Also note that for the groups T_d, O_h, the Cartesian rep transforms according to a single irrep, which means the photoluminiscent light will not be polarised. As such, it should be detected by both the detector in the $x - y$ plane and the detector along the z-axis, with halved intensity in the latter due to passing through a linear polariser. Furthermore, the lines in the $x - y$ polarisation and z polarisation should line up at equal energies, since each pair of lines corresponds to a single transition.

	e, $\left\lvert j=\frac{1}{2}, j_z=\pm\frac{1}{2}\right\rangle$	h-h, $\left\lvert j=\frac{3}{2}, j_z=\pm\frac{3}{2}\right\rangle$	lh, $\left\lvert j=\frac{3}{2}, j_z=\pm\frac{1}{2}\right\rangle$
C_{3v}	$E_{1/2}$	$E_{3/2}$ ($^1E_{3/2} \oplus {}^2E_{3/2}$)	$E_{1/2}$
C_{6v}	$E_{1/2}$	$E_{3/2}$	$E_{1/2}$
D_{3h}	$E_{1/2}$	$E_{3/2}$	$E_{5/2}$
D_{3d}	$E_{1/2,g}$	$E_{3/2,u}$ ($^1E_{3/2,u} \oplus {}^2E_{3/2,u}$)	$E_{1/2,u}$

Table 1: Irreps corresponding to electrons, heavy holes, and light holes, respectively, in several point groups. In the parentheses after an irrep label, its decomposition into conjugate representations is denoted if applicable.

	one hole	two holes
T_d	$F_{3/2}$	$A_1 \oplus E \oplus T_2$
O_h	$F_{3/2,u}$	$A_{1g} \oplus E_g \oplus T_{2g}$

Table 2: Transformation properties of one hole and two holes in a single energy level, respectively.

6.4 Predictions and their agreement with experiments

The predictions our model makes are the numbers of different emission lines between two exciton complexes. These lines should in theory be separated by fine-structure energy splitting, however, due to accidental degeneracy, some lines may not be resolvable in the experiment. Therefore, observing a lower number of lines than predicted does not necessarily contradict the assumed symmetry group, and more careful analysis of which lines probe the symmetry is needed to robustly disconfirm it.

6.4.1 Fermion transformation properties in different groups

The groups C_{3v}, C_{6v}, D_{3h}, and D_{3d} undergo splitting of the valence band into heavy holes and light holes at the Γ point, and therefore their exciton complexes are fully characterised by the single-fermion transformation properties. See Table 1 for the associated irreps as labelled by Altmann, [14].
Note that the electron and light-hole labels in D_{3h} are $E_{1/2}$ and $E_{5/2}$, respectively. This is interchanged in the analysis of Karlsson *et al.* [1, p. 14], which does not lead to different predictions.
The groups T_d and O_h have the heavy hole and light hole bands degenerate at the Γ point, where all holes transform according to a single irrep. Therefore, for these groups we list the transformation properties of both a single-hole state and a double-hole state, with the triple-hole state transforming equally to the single-hole state and the full energy level transforming according to the identity rep (see Sec. 5.2.3). See Table 2 for the associated irreps in the Altmann convention.

Exciton decay label		σ-polarised			z-polarised		
short	full	C_{3v}	D_{3h}	T_d	C_{3v}	D_{3h}	T_d
$X_{\bar{1}0}$	$X_{10} \rightarrow$ vac.	2	1	1	0	0	1
$X_{0\bar{1}}$	$X_{01} \rightarrow$ vac.	1	1	1	1	1	1
$X^+_{\bar{2}0}$	$X^+_{20} \rightarrow$ h-h	1	1	4	0	0	4
$X^+_{1\bar{1}}$	$X^+_{11} \rightarrow$ h-h	2	2	4	2	2	4
$X^+_{\bar{1}1}$	$X^+_{11} \rightarrow$ l-h	4	3	4	2	1	4
$X^+_{0\bar{2}}$	$X^+_{02} \rightarrow$ l-h	1	1	4	1	1	4
$X^-_{\bar{1}0}$	$X^-_{10} \rightarrow$ e	1	1	1	0	0	1
$X^-_{0\bar{1}}$	$X^-_{01} \rightarrow$ e	1	1	1	1	1	1
$2X_{\bar{2}0}$	$2X_{20} \rightarrow X_{10}$	2	1	6	0	0	6
$2X_{1\bar{1}}$	$2X_{11} \rightarrow X_{10}$	4	2	6	4	2	6
$2X_{\bar{1}1}$	$2X_{11} \rightarrow X_{01}$	6	3	6	2	1	6
$2X_{0\bar{2}}$	$2X_{02} \rightarrow X_{01}$	1	1	6	1	1	6
$2X^+_{\bar{3}0}$	$2X^+_{30} \rightarrow X^+_{20}$	1	1	4	0	0	4
$2X^+_{2\bar{1}}$	$2X^+_{21} \rightarrow X^+_{20}$	1	1	4	1	1	4
$2X^+_{\bar{2}1}$	$2X^+_{21} \rightarrow X^+_{11}$	4	3	4	2	1	4
$2X^+_{1\bar{2}}$	$2X^+_{12} \rightarrow X^+_{11}$	2	2	4	2	2	4
$2X^+_{\bar{1}2}$	$2X^+_{12} \rightarrow X^+_{02}$	1	1	4	0	0	4
$2X^+_{0\bar{3}}$	$2X^+_{03} \rightarrow X^+_{02}$	1	1	4	1	1	4

Table 3: The predicted number of different transitions between exciton complexes for the a priori assumed true group C_{3v}, the elevation supergroup D_{3h} as suggested by Karlsson *et al.*, and the only supergroup which also respects bulk symmetry, T_d. The short label for a decay identifies the initial complex and indicates which hole type recombines with a bar over the occupation number.

6.4.2 Number of lines for exciton and biexciton decays

We have found that D_{3d} gives equal predictions to C_{3v}, C_{6v} gives equal predictions to D_{3h}, and O_h gives equal predictions to T_d, and hence we omit D_{3d}, C_{6v}, and O_h from further analysis for brevity.

The data from Table 3 is compared to experimental data collected by Francesco Mattana, Luca Colavecchi, Gediminas Juska and Emanuele Pelucchi (Tyndall National Institute, University College Cork), which they shared with us together with their preliminary analysis. The dataset is to-be published, and will be referred to by the authorial initials MCJP. The authors have conducted correlation measurememts to identify specific peaks by their corresponding exciton transition. The experimental and analysis details will be included in their upcoming article.

In the experimental data, for specific transitions there seems to be variations in the spectrum, as if the QDs split into two sub-populations with different properties. Specifically, for $X_{\bar{1}0}$ and $X_{0\bar{1}}$, MCJP identify two separate characteristic spectra shown in Fig. 1. For one sub-population, the missing of one σ-polarised line for $X_{\bar{1}0}$ as noted by Karlsson *et al.* is reproduced. However, in this sub-population, a resolvable z-polarised peak is measured, contradicting the D_{3h} assumption and sug-

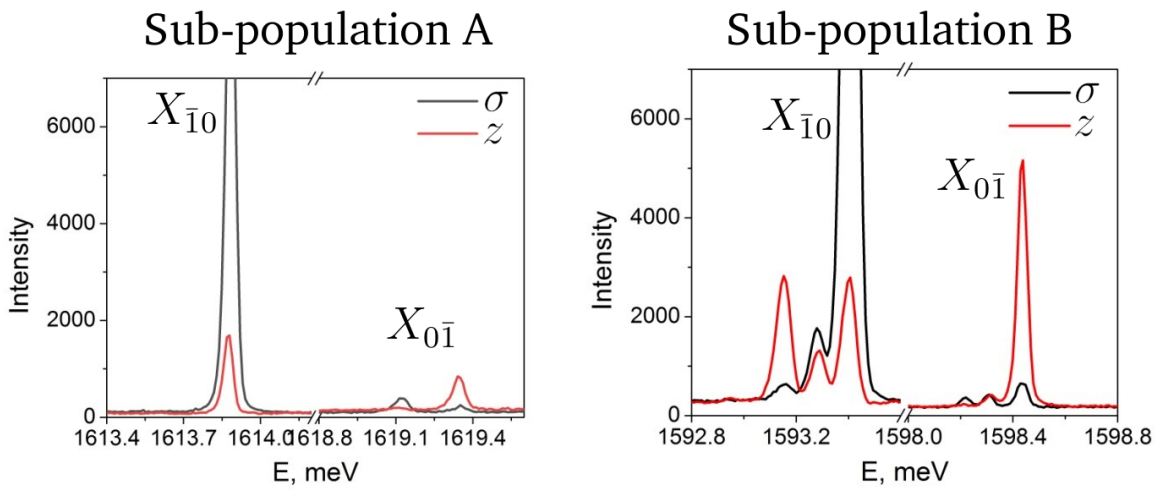

Figure 1: Spectra of two types of QDs in the neutral exciton decays. The σ and z-polarised spectra are colour-coded black and red, respectively.

gesting an elevation to the bulk symmetry T_d. The two most-resolvable lines in σ and z polarisation for $X_{0\bar{1}}$, conversely, contradict elevation to T_d, as their energies are inequal. The second sub-population matches neither of the analysed groups, as the number of peaks in both polarisations for $X_{\bar{1}0}$ and σ-polarisation for $X_{0\bar{1}}$ seems to increase.

The negatively charged exciton spectra are shown in Fig. 2. Both hole types feature a single strong line in both σ and z polarisation. For $X_{0\bar{1}}$, this agrees with the predictions of all analysed groups. However, for $X_{0\bar{1}}$, the z-polarised peak seems to probe the bulk symmetry T_d, as z-polarised transitions are forbidden in the structure symmetry. However, Karlsson *et al.* seem to have the z-polarised peak appear faintly, or not resolvable at all.

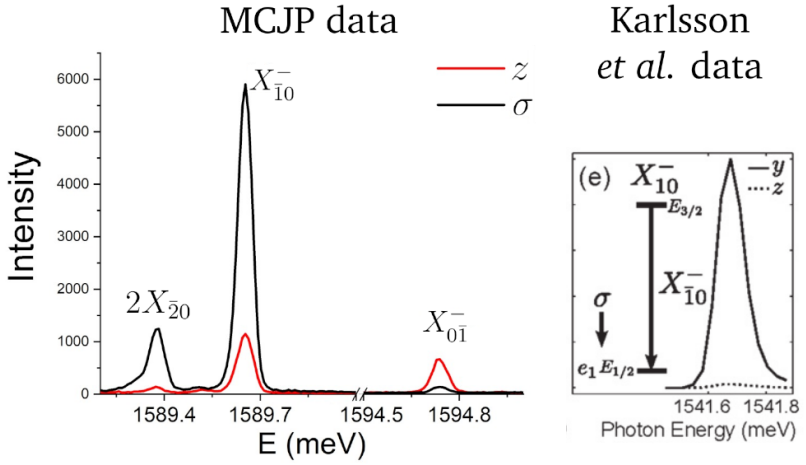

Figure 2: Spectrum of the negatively charged excitons, compared between the new MCJP dataset and the Karlsson dataset. Karlsson dataset plot taken from [1, Fig. 15 e)]

The spectra of positively charged excitons and biexcitons are shown in Fig. 3. For $2X^{+}_{\bar{2}1}$, 3 resolvable peaks with both σ and z-polarised components are always present, with the latter polarisation contradicting the predictions of C_{3v} and D_{3h}. In sub-population A a fourth peak, with both σ and z-polarised components, is usually present, but is not conclusively proven to be part of the complex by the MCJP correlation measurements. 4 peaks in both polarisations would be good evidence for elevating to bulk symmetry.
For $X^{+}_{\bar{1}1}$, three peaks are always certain in both sub-populations, with z-polarised components seemingly weakened and multiple added faint σ-polarised peaks occuring in B. The three z-polarised peaks contradict C_{3v} and D_{3h} predictions and are consistent with T_d for sub-population A, while the 4 σ-polarised and 2 resolvable z-polarised lines show agreement with C_{3v} for sub-population B.
For $X^{+}_{1\bar{1}}$, four strong lines with both σ and z components are present for both types, contradicting C_{3v} and D_{3h} and agreeing with T_d. However, the relative intensities of lines c, b, a disconfirm the assumption of emissions with no polarisation, since that predicts the z-polarised detector measuring the lines at half-intensity. Both populations here exhibit the dominance of the z-polarised component for lines c and b. Altogether, this constitues weak evidence for elevation to the bulk symmetry, conditioned by the presence of another mechanism which introduces z-polarisation bias. Interestingly, in the Karlsson *et al.* data, only two lines are detected in either polarisation, in agreement with both C_{3v} and D_{3h}, contradicting the bulk symmetry elevation, for a subpopulation of 15% of their QDs. Other QDs exhibited different spectra, typically with extra lines ([1, Fig. 19]), which suggest partial elevation to T_d.

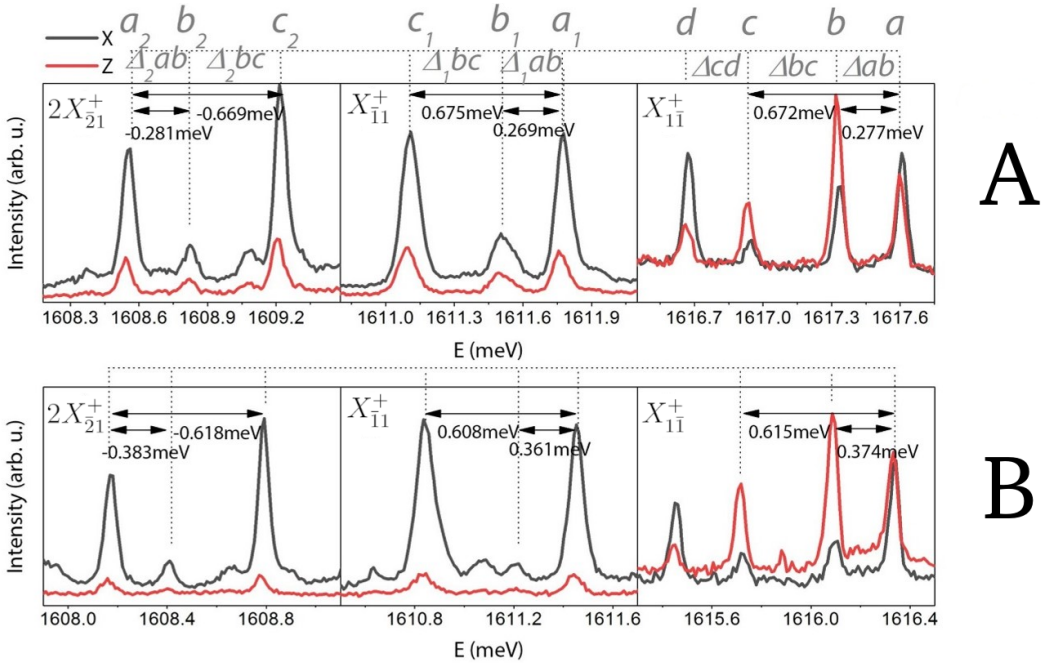

Figure 3: Spectrum of the positive biexciton $2X^{+}_{\bar{2}1}$ and the positive mixed-hole excitons $X^{+}_{\bar{1}1}$ and $X^{+}_{1\bar{1}}$. Two distinct sub-populations were identified, labelled A and B. Major peaks are identified by MCJP and their energy differences highlighted.

For other positively charged excitons and biexcitons, MCJP have no data. However, Karlsson *et al.* identified a single line for either polarisation for $2X^{+}_{2\bar{1}}$, in agreement with C_{3v} and disagreement with T_d. Similarly, $X^{+}_{1\bar{2}}$ had two σ-polarised lines and one z-polarised line, with another one predicted to overlap with a different peak, identified, in agreement with C_{3v}. For $X_{\bar{2}0}$, a single σ-polarised line was detected, seemingly in agreement with C_{3v}. However, activity in the z-polarised spectrum is faintly evident. Better-resolved measurement in the z-polarised spectrum could find evidence for weak elevation to the bulk symmetry.
The sectra of neutral biexcitons are shown in Fig. 4. MCJP were unable to conclusively identify all peaks in the $2X_{\bar{1}1}$ transition as belonging to it. Due to the ambiguous identification of lines and the unresolvability of the predicted large number of lines, the transition was not analysed here. Karlsson *et al.* note that the z-polarised peaks may be present but very weak due to the heavy-hole recombination [1, p. 16], and thus missing z-polarised lines do not constitute evidence against elevation to T_d. For the transition $2X_{\bar{2}0}$, a strongly resolvable z-polarised peak is measured, contradicting C_{3v} and D_{3h}. While T_d predicts 6 z-polarised peaks, it is possible that they are too tightly spaced to be resolvable, especially since the energy splitting may be reduced due to the approximate nature of elevating to the bulk within symmetry suppression theory.

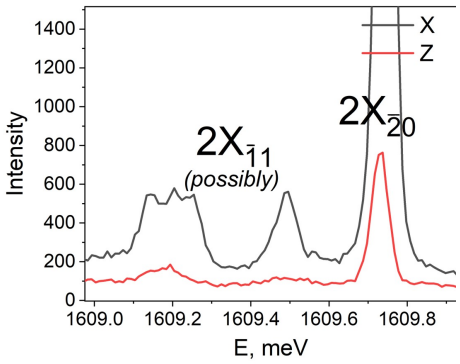

Figure 4: Spectrum of two neutral biexcitons.

7 Discussion of results

no agreement, too many lines for Td
for X1(1)+ the extra mechanism could be caused by the interfaces, which have an orientation!!! or the envelope function decoupling z from the cartesian rep!!!!!! because k will be slightly nonzero = outside of ground state, reinforcing structure symmetry with extra characters!!!!!
a mechanism picking the bulk symmetry elevation aside from the centre localisation (to explain karlsson discrepancy)

7.1 Agreement with C_{6v} is a coincidence

its a mathematical coincidence. C6v cannot be the group because fcc lattice. no other group agrees with experiment.

7.2 Symmetry outside of the Γ point

In the symmetry suppression model, we have assumed all excited fermions to have zero crystal momentum, which is necessary to use the "charged particles in a box" dynamics for the envelope functions. However, this is only an approximation based on the nature of the direct band-gap of InGaAs. For an excited fermion outside of the Γ point, the non-zero crystal momentum vector $\vec{k}$ breaks the wavefunction symmetry, as described by Dresselhaus in [12, Ch. 13]. In an interplay with the bulk symmetry, the true symmetry of the Hamiltonian $\hat{H}\left(\vec{k}\right)$ depends on the crystal momentum.
Since this effect breaks symmetry and does not elevate it, it is sufficient to test all subgroups of the Hamiltonian symmetry at Γ to see if the predictions for any of them match the experimental data. Obtaining such a group and finding the values of $\vec{k}$ in the Brillouin zone it corresponds to could hint at a possible effect which forces the excitons to have a non-zero crystal momentum.
acctually the envelope may just transform according to smth

7.3 mottness? spontaneous symmetries? what?

8 Conclusions

symmetry elevation is not a symmetry effect ater all :((

9 Acknowledgements

Our supervisor, collaborators, and my friends and others for their discussion, consultation, and support.

10 Bibliography

References

[1] Karlsson, K. F. *et al.* (2015), Spectral signatures of high-symmetry quantum dots and effects of symmetry breaking. *New Journal of Physics*, **17** 103017

[2] Karlsson, K. F. *et al.* (2010), Fine structure of exciton complexes in high-symmetry quantum dots: Effects of symmetry breaking and symmetry elevation. *Phys. Rev. B*, **81** 161307(R)

[3] Holsgrove, K. M. *et al* (2022), Towards 3D characterisation of site-controlled InGaAs pyramidal QDs at the nanoscale. *J Mater Sci*, **57** 16383–16396

[4] Bester, G., Zunger, A. (2005), Cylindrically shaped zinc-blende semiconductor quantum dots do not have cylindrical symmetry: Atomistic symmetry, atomic relaxation, and piezoelectric effects. *Phys. Rev. B*, **71** 045318

[5] Burt, M. G. (1992), The justification for applying the effective-mass approximation to microstructures. *J. Phys.: Condens. Matter*, **4** 6651. doi.org/10.1088/0953-8984/4/32/003

[6] Burt, M. G. (1999), Fundamentals of envelope function theory for electronic states and photonic modes in nanostructures. *J. Phys.: Condens. Matter*, **11** 53

[7] Hsiaw, H. C., Johnson, K. H., Lo, C. F., Adler, D. (1988), Valence and conduction band molecular-orbital topologies and the optical and electrical properties of gallium arsenide and silicon. *J. Non-Cryst. Solids*, **105** Iss. 1-2 101-106. doi.org/10.1016/0022-3093(88)90343-2

[8] Wigner, E. P. (1959), *Group Theory and Its Application to the Quantum Mechanics of Atomic Spectra* (transl. by Griffin, J. J.) (Exp. a. imp. ed.). Academic Press, New York and London. Library of Congress Catalog Card No. 59-10741 (Original work published in 1951)

[9] Landau, L. D., Lifshitz, E. M. (1977, repr. 1991 w. corrections), *Quantum Mechanics: Non-Relativistic Theory* (transl. by Sykes, J. B., Bell, J. S.) (3rd ed., revised a. enlarged). Pergamon Press, Oxford. ISBN 0-08-020940-8 (Translated from 4th ed. published in 1989)

[10] Goldberg, Y. A., Schmidt, N. M. (1996), *Gallium Indium Arsenide ($Ga_xIn_{1-x}As$)* in *Handbook Series on Semiconductor Parameters: Volume 2: Ternary And Quaternary III-V Compounds* (edited by Levinshtein, M., Rumyantsev, S., Shur, M.). World Scientific, London. ISBN 981-02-1420-0 (Set)

[11] Dresselhaus, M. S., Dresselhaus, G., Jorio, A. (2007), *Group Theory: Application to the Physics of Condensed Matter* (1st ed.). Springer Berlin, Heidelberg. doi.org/10.1007/978-3-540-32899-5

[12] Dresselhaus, M. S. (2002), *Applications of Group Theory to the Physics of Solids*. Massachusetts Institute of Technology.

[13] Biedenharn, L. C., Louck, J. D. Louck (2009), *Angular Momentum in Quantum Physics: Theory and Application (Encyclopedia of Mathematics and its Applications, Series Number 8)* (illustrated ed.). Addison-Wesley Publishing Company, Advanced Book Program. ISBN 0-201-13507-8

[14] Altmann, S. L., Herzig, P. (1994), *Point-Group Theory Tables*. Oxford: Clarendon Press